Journal of the Egyptian Society of Parasitology, Vol. 54, No. 3, December 2024
J. Egypt. Soc. Parasitol. (JESP), 54(3), 2024: 429– 439
Online: 2090-2549

THERAPEUTIC EFFICACY OF ARTEMISIA JUDAICA EXTRACT LOADED ON SILVER NANOPARTICLES IN EXPERIMENTALLY INDUCED MURINE TRICHINELLOSIS

By
MOSTAFA E. MOSTAFA[1], MORSY R. M. GENEEDY[2], AHMED M. A. MOHAMED[2], and FATMA M. EL-LESSY[3*]
Departments of Parasitology, Faculty of Medicine Al-Azhar University, Damietta[1], and Cairo[2,3], Egypt (*Correspondence: fatmamelessy@yahoo.com)

Abstract

Benzimidazole derivatives are frequently used to treat trichinellosis. However, drug resistance, adverse effects, and low bioavailability restrict their therapeutic use in treating *Trichinella* infections. The need for a novel, secure and efficient anti-trichinellosis treatment is therefore imperative. *Artemisia judaica* showed strong anthelmintic and antiprotozoal properties. The study evaluated the effectiveness of *A. judaica* extract compared with Albendazole alone or loaded on silver nanoparticles in trichinellosis infected mice. Mice were classified into 7 groups: GI: negative control, GII: positive control, GIII: infected treated with silver nanoparticles, GIV: infected treated with *Artemisia judaica* extract, GV: infected treated with albendazole, GVI: infected treated with *Artemisia judaica* extract loaded on silver nanoparticles and GVII: infected treated with albendazole loaded on silver nanoparticles. They were equally divided into two subgroups based on euthanasia time at 7th & 35th days post infection. Parasitological, immun- ological, and histopathological analyses were carried out to assess the efficacy of the treatment. *Artemisia judaica* extract loaded on silver nanoparticles treated mice induced a significant reduction in mean number of *T. spiralis* adults and larvae in infected mice, restored normal intestinal structure, and reduced pathogenic impact of infection by a significant decrease in GPx and SOD activities and immunomodulation of proinflammatory (TNF-α) and anti-inflammatory (IL-6, IL-10) cytokines. They may be useful as prospective trichinellosis treatment.

Keywords: *Artemisia judaica*, Albendazole, Silver nanoparticles, Cytokines, Trichinellosis.

Introduction

Trichinellosis is a widespread foodborne zoonotic illness brought on by a parasitic nematode belonging to the genus *Trichinella*, which is one of the top ten most prevalent foodborne parasites that can cause serious health issues. With an annual record of roughly 10,000 cases, it is regarded as a reemerging disease (Rawla and Sharma, 2023).

Humans contract infection by ingestion of raw or improperly cooked meat contaminated with *T. spiralis* larvae. *Trichinella* usually has two phases in their hosts: the intestinal (enteric) phase, which lasts for one to two weeks, and the muscular (parenteral) invasive phase (Darwish *et al,* 2022).

Clinically, *Trichinella* infection fluctuates from asymptomatic to fatal depending on the number of larvae and the site of invasion within the host body (Rosca *et al,* 2021). The *Trichinella* manifestation begins in the intestine with several gastric symptoms, including abdominal colic, nausea, vomiting, and diarrhea. These manifestations are due to the invasion of *T. spiralis* larvae into intestinal epithelial cells, where they mature, mate, and generate neonatal larvae 3-7 days beyond infection (El-kady *et al,* 2022).

In the parenteral phase, *Trichinella* larvae invade and encyst in striated muscle cells, remaining alive for one to several years, depending on the species, and the released larvae frequently induce widespread myalgia for up to 8 weeks, fever, significant eosinophilia, and malaise (Bai *et al,* 2022).

During human trichinellosis, a Th1/Th2 mixed immune response is produced, during the intestinal phase, Th1 is induced, and during the muscular phase, Th2 predominate. Th2- type immune responses mediated by IL-4, IL-5, IL-9, and IL-13, which in addition to IgE and IgG1 antibodies, and histamine released from mast cells lead to adult worm expulsion, reducing tissue damage and bolstering tissue regeneration (Wang *et*

al, 2020). Although Th2 cytokines are primarily responsible for the expulsion mechanisms, the pathways and mechanisms behind this process are yet unknown (Ding *et al,* 2017).

Benzimidazole analogues such as albendazole (ABZ), flubendazole, and mebendazole are anthelmintic drugs used to treat trichinellosis. Toxicity, acute hepatitis, nephronpathy, and encephalitis are among side effects reported (Codina *et al,* 2015). They have low bioavailability, low water solubility, and tissue absorption, as well as a moderate effect against encapsulated muscle larvae and a high resistance risk (Nada *et al,* 2018). Also, some of these drugs are prohibited during pregnancy and toddler age; others thought to be carcinogenic (Ahmed *et al,* 2022).

The need for novel and efficient medications to treat trichinellosis is thus imperative. *Artemisia judaica* (*A. judaica*) is a species of genus Artemisia of Asteraceae family. It is a perennial aromatic shrub, wildly distributed in Egypt mainly in Sinai Peninsula, the Red Sea coastal strip, Gebel Elba, and arround mountains (Ahmed *et al,* 2017).

A. judaica has strong antiviral, antibacterial, anthelmintic, antiprotozoal, and wound healing properties (Mokhtar *et al,* 2019; Marakhova and Emam, 2022; Mohammed *et al*, 2022; Qanash *et al,* 2023). The phytoconstituents-terpenoids and phenolics are the most prevalent ones associated with these biological actions (Goda *et al,* 2021).

The creation of nanoparticles and/or their combination with plant extract to improve their biological activities has recently attracted increased attention in the nanotechnology field. Silver nanoparticles (AgNPs) play an important role in this field due to their attractive physiochemical properties (Malik *et al,* 2023).

This study aimed to assess the efficacy of *A. judaica* ethanolic extract loaded on silver nanoparticles in treating murine trichinellosis by parasitological, immunological, antioxidant activity, and histopathological investigations.

Material and Methods

The study involved 68 male Swiss albino mice that were free of pathogens, weighing 22±5g and aged 6-8 weeks. Animals were obtained from the biological unit of the Theodor Bilharz Research Institute (TBRI) in Giza, Egypt, and experiments were conducted at Al-Azhar department of parasitology, during the period from April to July 2024. Mice were kept in 25°C air-conditioned rooms with unlimited access to water and a typical pellet diet.

Ethical consideration: Mice were treated following Al-Azhar University Guidelines rules in using animals in research that went with the Helsinki Declarations.

Parasite and inoculum preparation: *Trichinella spiralis* strain was isolated from infected albino mice that were raised laboratory in TBRI. Five weeks post-infection (PI), infected mice were sacrificed, dissected, and their muscles were digested in 200ml of distilled water contained 1% pepsin & 1% HCl for two hours, and the mixture was stirred continuously at 37°C by an electric stirrer. To get rid of coarse particles, the product was sieved via a 50-mesh/inch screen. After being gathered on a 200mesh/ inch sieve and cleaned with tap water twice, encysted larvae were suspended in 100ml of tap water in a conical flask.

Three sediment samples of 20µm were spread out on a slide, and larvae were counted using a binocular microscope (Khalifa *et al,* 2023). Mice were fasted for 12 hours before being orally infected with 250-300 larvae/ mouse using a blunt-nozzle tuberculin syringe. Each treatment was administered for three days at 3rd dpi to evaluate its effectiveness in the intestinal phase and for seven days at 26 dpi to evaluate its effectiveness in the muscular phase (Cameron *et al,* 2018).

Drugs: Albendazole (ABZ) was purchased from the Egyptian International Pharmaceutical Industries Co. A tablet of 100mg was mixed in 50ml of filtered water and given orally in dosage of 50mg/kg/day (Abou Rayia *et al,* 2017).

Artemisia judaica extract preparation: After being verified, the aerial portions of the *A. judaica* plant were allowed to air dry for a week at room temperature in shade before being manually ground into a fine powder. 200g of *A. judaica* were macerated twice with 300mL of 95% ethanol for 48 hours at 25°C to create the crude ethanolic extract, and dried in a rotary evaporator at 40°C with reduced pressure. *A. judaica* crude extract (16g) was obtained by vacuum-concentrating the mixed extracts (Mokhtar *et al,* 2019), kept at 4°C, and used to prepare a 200 mg/kg dosage for mouse trials of the dried extract.

Phenolic and flavonoids detection: Phenolic and flavonoid contents of the extract were estimated qualitatively and quantitatively. Using Folin-ciocalteu assay, with Gallic acid as a reference, total *Artemisia* extract phenolic content was measured spectrophotometrically. At λ 630nm, Milton Roy Spectronic 1,201 UV/Vis Spectrophotometer (Houston, TX, United States) was used to record UV absorbances in triplicate against each blank. By Gallic acid equivalents (mg GAE/gdry extract), outcome was determined with Quercetin as a reference, and AlCl3 technique quantified total flavornoid concentration. At λ 510nm, UV absorbance was measured in triplicate using a Milton spectrophotometer against a blank. Quercetin equivalent/gm of dry extract (mg QE/g) expressed outcome.

Biosynthesis and characterization of silver nanoparticles: To make a 1 mM silver nitrate solution, 0.017g of AgNO3 was dissolved in 100 ml of double-distilled water. Ratio of plant extract to silver nitrate was 1:9 (v/v). A magnetic stirrer was used to heat mixture and agitate it between 60 & 80°C at 300 rpm. A reddish-brown coloration of the mixture between 10 minutes and an hour indicated nanoparticles development. The green nanoparticles were separated by centrifugation for 45 minutes at 15,000 rpm. Albendazole was loaded on silver nanoparticles as followed: 1mg of silver nanoparticles was dissolved in 10ml of distilled water & 1mg of ABZ powder was added. It was put on a magnetic stirrer for 24hrs, concentrated, and dried by a rotary evaporator to prepare theapeutic doses. The stock was stored in a cool, dry, and dark place (Al-Otibi *et al,* 2021).

Transmission electron microscope (TEM) imaging confirmed the liquid structure of the synthesized nanoparticles. Following the manufacturer directions, the nanoparticles were purified, and the pure biosynthesized AgNPs were characterized at 200-800nm using a UV-visible spectrophotometer (Shimadzu, Tokyo, Japan). The DLS technique that computed the PDI and Z-average assessed the colloidal stability of nanoparticles and identify their particle size distribution.

Animals: A total of 68 mice were divided into seven groups: GI (n=8): negative control (neither infected nor treated), GII: 10 positive control (infected non-treated), GIII: 10 infected treated with silver nanoparticles in a dose of 50mg/kg, GIV: 10infected treated with *A. judaica* extract in a dose of 200-mg/kg, GV: 10 infected treated with ABZ in a dose of 50mg/kg, GVI:10 infected treated with *A. judaica* extract loaded onto silver nanoparticles in a dose of 200mg/kg, and GVII: 10 infected treated with ABZ loaded on silver nanoparticles at a dose of 2mg /ml/ mouse orally. Each group was divided into two equal subgroups. SGA: To assess medications impact on intestinal phase of mice euthanized 7 days PI. SGB: To assess medications impact on muscular phase of mice euthanized 35 days PI.

Blood samples: After 48hrs of last dose, mice were euthanized under isoflurane inhalation and decapitated, samples were obtained, spun at 2000rpm for 10minutes to separate sera, and stored at -20°C until used to measure parameters.

Efficacy of treatment was assessed by parasitological analysis: After dissecting mice, the intestine was removed and sliced into small pieces. Mice were cleaned, put in 10 ml of normal saline at 37°C for 4hrs, and repeatedly washed until the gut was clear. Fluid was collected and centrifuged at 1000 rpm for ten minutes, supernatant was deca-

nted and sediment was reconstructed in few saline drops and examined drop by drop under a dissecting microscope. Mean number of adults/mouse was counted. Reduction rate was calculated using the following formula:

Worm reduction % = (mean number of parasites in positive control - mean number in treated mice/ mean number of parasites in positive control x100).

Using the pepsin digestion procedure, muscle larvae were retrieved (Dunn and Wright, 1985). Under a microscope, the collected larvae were counted by a McMaster counting chamber and larval number/gram of digested carcass was parasite burden.

Immunological parameters: ELISA kits (Elabscience Bionovation Inc., USA; Catalog No.: E-AB-22159, E-AB-F12070, & E-AB-F1197E) were used to measure serum levels of TNF-α, IL-6, & IL-10, respectively, after the manufacturer's instructions.

Antioxidant parameters: ELISA kits (Biodiagnostic Co., Giza, Egypt) were used to measure antioxidant enzyme activities (glutathione peroxidase (GPx) and superoxide dismutase (SOD)) in the serum of the mice after the manufacturer's instructions.

Histopathological examination**:** Small intestinal sections of all mice sacrificed at 7 dpi and muscle specimens were collected from the intestine, and skeletal muscles of mice sacrificed at 35th dpi were fixed in 10% formal saline, dehydrated in ethanol, washed with xylol, paraffin-embedded, sectioned at 5µm thickness, and stained with hematoxylin and eosin. Intestinal tissue inflammation degree was measured and scored on a scale of 0 to 3 (0, normal; 1, minimal infiltration; 2, moderate; 3, marked), and villous changes with broadening, fusion, and blunting (normal, minimal, moderate, or marked).

The encysted larval number per low-power field ×100 (+1 ≤ 1 larva; +2 = 2-10; +3 >10) and pericapsular inflammatory infiltrate (normal, minimal, moderate, & marked) scored the muscle alterations.

Statistical analysis: **S**oftware IBM-SPSS 22 (IBM-SPSS Inc., Chicago, IL, USA) was used to analyze coded and computerized data. Means, medians, ranges, frequencies, percentages, and standard deviations are examples of descriptive data. Continuous variables were checked for normality using Shapiro-Wilk test, and variables with more than two categories were examined for mean differences by ANOVA test. A P value <0.05 was considered significant.

Results

Artemisia judaica extract had an average phenolic content of 48.6± 1.3mg Gallic acid/1g dry extract and an average flavonoid content of 57.3± 2.1mg quercetin/1g dry extract. Comparing all treated SGs A to untreated infected subgroup (GIIA), a significant decrease in the mean adult worm count was (P< 0.001). GVIA and GVIIA given *A. judaica* and ABZ loaded on silver nanoparticle therapy respectively, showed less mean count of adults (21.1±1.8 &16.5±0.8) and efficacy (84.7% & 88%), respectively.

With 35.3% efficacy, silver nanoparticle treatment (GIIIA) considerably (P =0.041) reduced mean number of adults (89.1±3.2) compared to the untreated infected subgroup (GIIA). The mean count in (GVA), treated with ABZ, was 32.1±3.4 showed 76.7% efficacy, but mean count in (GIVA), *A. judaica* treated (51.8±4.7) showed 62.4% efficacy without significance (P =0.101).

Treated muscular phase, mean larval number/gram was significantly lower in SGBs than in positive control (GIIB). Mice received *A. judaica* (GVIB) and ABZ (GVIIB) loaded on silver nanoparticles showed least larval mean count (27.3±1.5 & 31.7± 2.4), with efficacy rates of 78.4% &75%, respectively, followed by (GIVB) *A. judaica* treated (49.7±3.1) with 60.7% efficacy. ABZ treated, larval mean count (53.2 ±1. 3), with 58% efficacy. Least reduction was in (GIIIB) silver nanoparticles with efficacy of 41.7%

Cytokines in sera of mice sacrificed on 7th & 35th dpi were significantly up-regulated in positive control at both time phases as compared to negative one. TNF-α was down-regulated in all treated mice on 7th & 35th days

PI compared to GII (P< 0.001), in all treatment mice IL-6 was higher (P < 0.001), and IL 10 showed up-regulated compared to GII (P < 0.001).

Positive control was higher (P < 0.001) glutathione peroxidase, and superoxide dismutase levels than negative control showed intense oxidative stress. GII, oxidative stress levels were much lower in all treated mice. *A. judaica* (GVI) & ABZ (GVII) loaded on silver nanoparticles showed least activities and back to nearly negative values. *A. judaica* treated infected mice didn't show significant (P=0.151 & =0.324, respectively).

Details were given in tables (1, 2, & 3) and figures (1, 2, 3, 4, 5, 6, 7, & 8).

Table 1: Effect of treatment on the adult count/ml at 7 dpi:

Adult count/ml at 7 dpi	Mean ± SD	P-value**			Reduction
GIA (n=4)		2 vs. 3=0.041	3 vs. 6<0.001	6 vs. 7=0.212	
GIIA (n=5)	137.7 ± 8.5	2 vs. 4=0.024	3 vs. 7<0.001		
GIIIA (n=5)	89.1 ± 3.2	2 vs. 5=0.001	4 vs. 5=0.101		35.3%
GIVA (n=5)	51.8 ± 4.7	2 vs. 6<0.001	4 vs. 6=0.024		62.4%
GVA (n=5)	32.1 ± 3.4	2 vs. 7<0.001	4 vs. 7=0.017		76.7%
GVIA (n=5)	21.1 ± 1.8	3 vs. 4=0.495	5 vs. 6=0.065		84.7%
GVIIA (n=5)	16.5 ± 0.8	3 vs. 5=0.011	5 vs. 7=0.053		88.0%
P-value*	< 0.001				< 0.001

*ANOVA compared mean difference between groups **Pairwise comparison, post-hoc test with Tukey's correction.

Table 2: Effect of treatment on larva count/gm at 35 dpi:

Larva count/gm at 35 dpi	Mean ± SD	P-value**			Reduction
GIB (n=4)		2 vs. 3=0.034	3 vs. 6<0.001	6 vs. 7=0.624	
GIIB (n=5)	126.6 ± 4.2	2 vs. 4=0.016	3 vs. 7<0.001		
GIIIB (n=5)	73.8 ± 4.2	2 vs. 5=0.017	4 vs. 5=0.824		41.7%
GIVB (n=5)	49.7 ± 3.1	2 vs. 6<0.001	4 vs. 6=0.031		60.7%
GVB (n=5)	53.2 ± 1. 3	2 vs. 7<0.001	4 vs. 7=0.033		58%
GVIB (n=5)	27.3 ± 1.5	3 vs. 4=0.042	5 vs. 6=0.067		78.4%
GVIIB (n=5)	31.7 ± 2.4	3 vs. 5=0.044	5 vs. 7=0.072		75.0%
P-value*	< 0.001				< 0.001

Table 3: Effect of Treatment on Histological Examination during Muscular Phase:

SGB	Pericapsular Infiltrate				Muscle larvae count		
	Normal	Minimal	Moderate	Marked	+1 (≤ 1)	+2 (2-10)	+3 (> 10)
GIB	4 (100%)	0 (0%)	0 (0%)	0 (0%)	4 (100%)	0 (0%)	0 (0%)
GIIB	0 (0%)	0 (0%)	2 (40%)	3 (60%)	0 (0%)	2 (40%)	3 (60%)
GIIIB	0 (0%)	0 (0%)	3 (60%)	2 (40%)	0 (0%)	3 (60%)	2 (40%)
GIVB	0 (0%)	0 (0%)	4 (80%)	1 (20%)	1 (20%)	3 (60%)	1 (20%)
GVB	0 (0%)	1 (20%)	3 (60%)	1 (20%)	0 (0%)	4 (80%)	1 (20%)
GVIB	2 (40%)	1 (20%)	2 (40%)	0 (0%)	3 (60%)	1 (20%)	1 (20%)
GVIIB	1 (20%)	3 (60%)	1 (20%)	0 (0%)	2 (40%)	2 (40%)	1 (20%)
P-value*		= 0.003			= 0.044		

*Monte Carlo exact test was used to compare the difference in frequency between groups.

Discussion

Benzimidazole derivatives are frequently used to treat trichinellosis. However, they do not address both phases of illness (Ebrahim *et al,* 2024). Drug resistance, toxicity, adverse effects, and low bioavailability also restrict their therapeutic use in treating *Trichinella* infections (Fahmy and Diab, 2021).

The need for a novel, secure and effective anti-trichinellosis therapyu is imperative. In earlier studies, *A. judaica* showed strong anthelmintic and antiprotozoal properties. More attention was paid to the nanoparticles and their combination with plant extract to improve biological activities in the nanotechnology (Malik *et al,* 2023).

In this study, *A. judaica* extract showed an average phenolic content of 48.6±1.3mg, Gallic acid/1g dry extract and an average flavonoid of 57.3±2.1mg quercetin/1g dry extract. This agreed with Ahmed *et al.* (2023), who found that plant has high phenolic and flavonoid compounds levels (52.6±3.1mg GAE/g and 64.5±3.1mg QE/g, respectively). Also, it agreed with Qanash *et al.* (2023), who found that aerial parts *A. judaica* were very rich in phenolic and flavonoid compounds with various therapeutic properties.

When compared to positive control, mice, showed a marked decrease in parasitic burden in their intestine and muscular regions. In intestinal phase, best response (84.7%), and (88%) efficacy were caused by *A. judaica* extract and ABZ loaded on silver nanoparticles, but both substances alone decreased parasite burden with 62.4% & 76.7% efficiency, respectively. ABZ anti-trichineosis was reported (Huang *et al,* 2020; El-Wakil *et al,* 2021; Abo Maged *et al,* 2023) with varied effectiveness degrees due to differences in dosage, and duration. *A. judaica* extract against *T. spiralis* has not studied.

Blastocystosis, giardiasis, cutaneous leishmaniasis, and cryptosporidiosis are well treated with *A. judaica* globally (Mokhtar *et al,* 2019; Abd-Elhamid *et al,* 2021; Najm *et al,* 2021; Ahmed *et al,* 2023). Also, *A. judaica* extract treated schistosomiasis (Mohammed *et al,* 2022).

In the present study, *A. judaica* extract and ABZ loaded on silver nanoparticles showed the greatest decrease in parasite burden in muscles (78.4% and 75%, respectively), followed by *A. judaica* extract (60.7%) and the least was ABZ (58%). This was lower than that of Nassef *et al.* (2018), who reported (99.1%) reduction of *T. spiralis*. The present study showed that plant extracts were not as effective against encysted larvae as adults. This could be due to the fact that *Trichinella* larvae encysted in muscle tissues is less possible as cyst's vulnerability to chemotherapies decreased with infection duration.

In the present study, TNF-α, IL-6, and IL-10 measured in sera of sacrificed mice of at the 7^{th} &35^{th} dpi were significantly up-regulated in positive control compared to negative control at both time phases. TNF-α was down-regulated in all treated mice on 7^{th} & 35^{th} dpi as compared to positive control. This agreed with Naguib *et al.* (2023), who found that positive control had significantly higher TNF-α levels than negative ones, but treated mice had significantly lower TNF-α levels that mimicked by infection. Abdullatif *et al.* (2021) found that silver nanoparticles prevented TNF-α production.

In the present study, IL-6 concentration significantly increased in positive control as compared to negative one ($P < 0.001$). IL-6 was elevated in all treated mice at 7^{th} & 35^{th} dpi ($P < 0.001$) as compared to positive control. Farrag *et al.* (2021) found that the mice had higher levels of IL-6 than positive controls. Artemisia down regulated IL2 & IFN-γ, but up-regulated IL-4, IL-10 & anti-inflammatory activity (Huang *et al*, 2022).

The present study showed that IL-10 level was significantly higher in positive control than in negative ones. IL-10 increased in the ABZ-treated mice but was lower than in *A. judaica* extract-treated mice. Also, mice treated with *A. judaica* extract and ABZ loaded on silver nanoparticles showed greatest elevation of IL-10. This agreed with Mohamed *et al.* (2019), who found that *L. donovani* infected mice treated with silver nanoparticles compared to Pentostam® showed IL-10 increased levels after 3 weeks. But, this disagreed with Naguib *et al.* (2023), who found a significant decrease in IL-10 in treated mice. Also, Jari and Yousif (2020), reported that echinococcosis treatment reduced IL-10 level. The increased IL-10 production is a characteristic of hosts' immune response in helminth-induced immunoregulation (Ilic *et al,* 2021). Changed in cytokine profile may be due to the *Trichinella* capacity to produce immunostimulation and immunomodulation of either innate or adaptive immune system components.

The present study showed that the antioxidant enzymes GPxs & SOD levels significantly increased in positive control, suggesting intense oxidative stress during trichinellosis. This agreed with both Gabrashanska *et al.* (2019) and Hassan *et al.* (2024), they reported that post treatment sera of infected mice showed marked reduced levels of antioxidant enzymes. This agreed with Soliman *et al.* (2013) and Elmehy *et al*. (2021), who noted decreased in activity of glutathione-S-transferase, lactate dehydrogenase, and SOD in both stages of trichinellosis. However, El-

Hamed *et al.* (2024) found that the superoxide dismutase 3 and glutathione (GSH) levels were significantly higher in infected treated mice and positive control. They added that cytokines release and ROS production by host as a defence mechanism are most likely mechanisms underlying tissue damage produced by trichinellosis.

In the present study, *T. spiralis* infection induced significant inflammation in the intestinal and muscle tissues. Inflammatory infiltrates with villi broadening were found intestinal positive control, and improved post *A. judaica* extract and ABZ, loaded on silver nanoparticles. This agreed with many authors (Abou Rayia *et al*, 2017; Nassef *et al*, 2018; Elguindy *et al*, 2019; El-Wakil *et al*, 2023).

In the present study, in the positive control muscular phase showed numerous encysted larvae with marked infiltration of capsule by inflammatory cells. This agreed with Sarhan *et al*, (2021); El-Wakil *et al*. (2021) and Abo Maged *et al*. (2023). The present reduction in inflammatory score, villous changes in intestine, and fewer degenerated larvae in muscles indicated histopathological improvement in trichinosis. Matar *et al*. (2023) reported that ABZ showed a stronger effect in the enteral phase than in the parenteral phase and that *A. judaica* extract was more effective in muscular phase than in intestinal one. The therapy reduced the number of *T. spiralis* adults and larvae in infected mice, restored normal intestinal structure, and reduced the parasite pathogenic impact.

Conclusion

Artemisia judaica extract modulates the pathological response and immune defense mechanisms of the infected host, making it a safe and effective natural alternative to ABZ in treating *T. spiralis* infections. The antiparasitic, anti-inflammatory, and antioxidant properties were enhanced when loaded on silver nanoparticles. They proved to be useful in trichinellosis treatment.

Authors' declaration: They declared that neither have any conflict of interest nor received any funds.

Authors' contributions: All authors equally shared in theoretical and practical studies. They wrote, revised the manuscript and approved its publication

References

Abd-Elhamid, TH, Abdel-Rahman, AM, Mahmoud, AR, Allemailem, KS, Almatroudi, A, *et al,* 2021: A complementary herbal product for controlling giardiasis. *Antibiotics* 10:477. doi: 10.3390/ antibiotics10050477.

Abdel Hamed, EF, Taha, AA, Abdel Ghany, S M, Saleh, AA, Fawzy, EM, 2023: Acetazolamide loaded-silver nanoparticles: A potential treatment for murine trichinellosis. J. Helminthol. 97:e1-10.

Abdullatif, AA, Alsharidah, M, Al Rugaie, O, Tawfeek, HM, Tolba, NS, 2021: Silver nanoparticle- coated ethyl cellulose inhibits tumor necrosis factor-α of breast cancer cells. Drug Des. Devel. Ther. 15:2035-46.

Abo Maged, AI, Metwally, KM, El-Menyawy, HM, Hegab, F, El-Wakil, ES, 2023: Assessment of the potential prophylactic and therapeutic effects of kaempferol on experimental *Trichinella spiralis* infection. J. Helminthol. 97:36-40.

Abou Rayia, DM, Saad, AE, Ashour, DS, Oreiby, RM, 2017: Implication of artemisinin nematocidal activity on experimental trichinellosis: in-vitro and in-vivo studies. Parasitol. Inter. 66, 2:56-63.

Ahmed, ES, Mabrouk, DM, Hassanane, MM, Khalil, WKB, 2017: Protective effect of *Artemisia judaica* against doxorubicin-induced toxicity in mice. Ann. Res. Rev. Biol. 18:1-10.

Ahmed, SA, Eltamany, EE, Nafie, MS, Elhady, SS, Karanis, P, *et al,* 2023: Anti-*Cryptosporidium parvum* activity of *Artemisia judaica* L. and its fractions: in vitro and in vivo assays. Front. Microbiol. 14:1193810.doi: 10.3389/fmicb. 2023.1193810

Al-Otibi, F, Al-Ahaidib, RA, Alharbi, RI, Al-Otaibi, RM, Albasher, G, 2021: Antimicrobial potential of biosynthesized silver nanoparticles by *Aaronsohnia factorovskyi* extract. Molecules 26:130-8.

Bai, H, Tang, B, Qiao, W, Wu, X, Liu, M, *et al,* 2023: The prevalence of *Trichinella spiralis* in domestic pigs in China: A systematic review and meta-analysis. Animals 12, 24:35-53.

Cameron, SJ, Hosseinian, F, Willmore, WG, 2018: Current overview of the biological and ce-

llular effects of nanosilver. Int. J. Mol. Sci. 19: 20-30.

Codina, AV, García, A, Leonardi, D, *et al,* 2015: Efficacy of albendazole: β-cyclodextrin citrate in the parenteral stage of *Trichinella spiralis* infection. Inter. J. Biol. Macromol. 77:203-6.

Darwish, AMM, Selim, MA, Mostafa, NES, Abdelhameed, RM, Fawzy, EM, 2022: General overview about *Trichinella* and trichinellosis. NeuroQuantol. 20, 16:43-60.

Ding, J, Bai, X, Wang, X, Shi, H, Cai, X, *et al,* 2017: Immune cell responses and cytokine profile in intestines of mice infected with *Trichinella spiralis*. Front Microbiol. 8:2069. doi: 10. 3389/fmicb. 02069

Dunn, IJ, Wright, KA, 1985: Cell injury caused by *Trichinella spiralis* in the mucosal epithelium of B10A mice. J. Parasitol. 71, 6:757-66.

Ebrahim, YA, Elkhawass, EA, Nabil, ZI, El-Shenawy, NS, 2024: A mini review of new potential therapeutic strategies against trichinellosis Egypt. Acad. J. Biol. Sci. (B. Zool.) 16, 1:177-89.

Elguindy, DA, Ashour, DS, Shamloula, MM, Aboul Assad, IA, 2019: Preliminary study on the role of toll-like receptor-4 antagonist in treatment of *Trichinella spiralis* infection. Tanta Med. J. 47, 2:52-61.

El-Hamed, A, Abd-Rabou, A, Faramawy, A, 2022: Therapeutic efficacy of curcuma and pomelo loaded chitosan nanoparticles in intestinal murine trichinellosis. Egypt. J. Chem. 65, 2:551-64.

El-Hamed, WA, Abdelaziz, YA, Amer, NA, 2024: Therapeutic efficacy of *Zingiber officinale* loaded chitosan nanoparticles in intestinal murine trichinellosis. Egypt. J. Chem. 67, 8:269-83.

El-Kady, AM, Abdel-Rahman, IAM, Sayed, E, *et al,* 2022: A potential herbal therapeutic for trich-inellosis. Front. Vet. Sci. 9:970-327.

Elmehy, DA., Hasby, MAS, El Maghraby, G M, *et al,* 2021: Niosomal versus nanocrystalline ivermectin against different stages of *Trichinella spiralis* infection in mice. Parasitol. Res. 120, 7: 2641-58.

El-Wakil, ES, Abdelmaksoud, HF, Abou-Shousha, TS, Ghallab, MMI, 2021: Evaluation of *Annona muricata* (Graviola) leaves activity against experimental trichinellosis: In vitro and in vivo studies. J. Helminthol. 95, 1:e53.

El-Wakil, ES, Khodear, GA, Ahmed, HES, Ibrahim, GIK, Hegab, F, *et al,* 2023: Therapeutic efficacy of albendazole and berberine loaded on bovine serum albumin nanoparticles on intestinal and muscular phases of experimental trichinellosis. Acta Trop. 241:106896.

Fahmy, AM, Diab, TM, 2021: Therapeutic efficacy of Albendazole and Mefloquine alone or in combination against early and late stages of infection in mice. Helminthologia 58, 2:179-87.

Farrag, HMM, Huseein, EAM, Abd El-Rady, NM, *et al,* 2021: The protective effect of *Lactobacillus acidophilus* on experimental animals challenged with *Trichinella spiralis*, new insights on their feasibility as prophylaxis in *Trichinella spiralis* endemic area. Ann. Parasitol. 67, 2: 195-202.

Gabrashanska, M, Petkova, S, Teodorova, S E, 2019: The antioxidant status in *Trichinella spiralis*-infected rats, improved by selenium supplementation. Open J. Chem. 5, 1:1-8.

Goda, MS, Nafie, MS, Awad, BM, Abdel-Kader, MS, Ibrahim, AK, *et al,* 2021: In vitro and in vivo studies of anti-lung cancer activity of *Artemesia judaica* L. crude extract combined with LC-MS/MS metabolic profiling, docking simulation and HPLC-DAD quantification. Antioxidants (Basel, Switzerland) 11:11. doi: 10.3390/ antiox11010017.

Hassan, ZR, El-Sayed, S, Zekry, K.M, *et al,* 2024: Impact of atorvastatin and mesenchymal stem cells combined with ivermectin on murine trichinellosis. Parasitol. Res. 123:57. https://doi. org/10.1007/s00436-023-08077-x

Huang, H, Yao, J, Liu, K, Yang, W, Wang, G, *et al,* 2020: Sanguinarine has anthelmintic activity against the enteral and parenteral phases of *Trichinella* infection in experimentally infected mice. Acta Trop. 201, 1:105226-34.

Huang, K, Chen, Y, Liang, K, Xu, X, Jiang, J, *et al,* 2022: Review of the chemical composition, pharmacological effects, pharmacokinetics, and quality control of *Boswellia carterii*. Evid-based Complement. Alter. Med. 66:27104.

IBM_SPSS, 2012: Statistical Package for Social Science. Ver. 24. Standard version. Copyright © SPSS Inc., NY, USA.

Ilic, N, Kosanovic, M, Gruden-Movsesijan, A, Glamoclija, S, Sofronic-Milosavljevic, L, *et al,* 2021: Harnessing immunomodulatory mechanisms of *Trichinella spiralis* to design novel nanomedical approaches for restoring self-tolerance in autoimmunity. Immunol. Lett. 238:57-67.

Jari, SD, Yousif, JJ, 2020: The effectiveness of silver nanoparticles loaded with albendazole,

mebendazole drugs in the level of some immunological markers in male albino mice infected with hydatid cyst. Biochem. Cell. Arch. 20, 2:34-9.

Khalifa, MM, Ramadan, RM, Youssef, FS, Auda, HM, El-Bahy, MM, *et al,* 2023: Trichinocidal activity of a novel formulation of curcumin-olive oil nanocomposite in vitro. Vet. Parasitol. Reg. Stud. Repts. Jun: 41:100880.doi: 10.1016/j.

Malik, S, Muhammad, K, Waheed, Y, 2023: Nanotechnology: A revolution in modern industry. Molecules 28:661-8.

Marakhova, AI, Emam, EM, 2022: A study of active medicinal plant (Artemisia judaica) against Staphylococcus aureus. Clin. Res. Clin. Trials 5:1-7.

Matar AM, Kora MA, Shendi SS, 2023: Evaluation of the therapeutic effect of *Olibanum* extract against enteric and intramuscular phases of trichinosis in experimentally infected mice. J. Helminthol. 97:e1-12

Mohamed, ST, Sulaiman, HH, Kamal, SB, Aja, HA, 2019: Effect of *Fusarium graminarum* silver-nanoparticles on IL-10 and INF cytokines levels in the mice by *Leishmania donovani* in vivo. IJB 18, 2:106-15.

Mohammed, HA, Qureshi, KA, Ali, HM, Alomar, MS, Khan, O, *et al,* 2022: Bio-evaluation of the wound healing activity of *Artemisia judaica* L. as part of the plant's use in traditional medicine; phytochemical, antioxidant, anti-inflammatory, and antibiofilm properties of the plant's essential oils. Antioxidants 11:332. doi:10.3390/antiox11020332/s1.

Mokhtar, AB, Ahmed, SA, Eltamany, EE, Karanis, P, 2019: Anti-*Blastocystis* activity in vitro of Egyptian herbal extracts (family: Asteraceae) with emphasis on *Artemisia judaica.* Int. J. Environ. Res. Pub. Hlth. 16:1555. doi: 10.3390/ijerph16091555.

Mostafa, EM, Ahmed, MS, Hassan, SS, 2020: Comparison of different techniques and stains for direct diagnosis of *Trichinella spiralis*. Microbes Infect. Dis. 1, 3:199-208.

Nada, S, Mohammad, SM, Moad, HS, El-Shafey, MA, *et al,* 2018: Therapeutic effect of *Nigella sativa* and ivermectin versus albendazole on experimental trichinellosis in mice. JESP 48, 1: 85-92.

Naguib, MM, El Hamshary, AS, Baoumi, IR, *et al,* 2023: Therapeutic efficacy of lactoferrin loaded on nano-particles in *Trichinella spiralis* infection in mice. JESP 53, 3:519-29.

Najm, M, Hadighi, R, Heidari-Kharaji, M, Alipour, M, Hajizadeh, M, *et al,* 2021: Anti-leishmanial activity of *Artemisia persica, A. spicigera*, and *A. fragrance* against *Leishmania major.* Iran. J. Parasitol. 16:464-73.

Nassef, NE, Moharm, I, Atia, AF, *et al*, 2018: Therapeutic efficacy of chitosan nanoparticles and albendazole in intestinal murine trichinellosis. JESP 48, 3:493-502.

Qanash, H, Bazaid, AS, Aldarhami, A, *et al,* 2023: *Trichinella spiralis* infection. In: StatPearls [Internet]. StatPearls Publishing.

Rawla, P, Sharma, S, 2023: *Trichinella spiralis*. In: StatPearls [Internet]. StatPearls Publishing.

Rosca, EC, Tudor, R, Cornea, A, Simu, M, 2021: Central nervous system involvement in trichinellosis: A systematic review. Diagnostics 11, 6:945-52.

Sarhan, M, Etewa, S, Al-Hoot, A, Arafa, S, Shokir, R, *et al,* 2021: stem cells as a potential therapeutic trend for experimental trichinosis. PUJ 14, 2:151-61.

Soliman, NA, Omar, RE, Nasr, HE, Eltantawy, AF, Salama, AM, 2023: Antacids as aluminum hydroxide and magnesium hydroxide effect on trichinosis: Experimental study. JESP 53, 1:115-22.

Wang, N, Bai, X, Tang, B, Yang, Y, Wang, X, *et al,* 2020: Primary characterization of the immune response in pigs infected with *Trichinella spiralis.* Vet. Res. 51, 1:17-22.

Explanation of figures

Fig. 1: TNF-α (pg/ml) levels between groups.
Fig. 2: IL-6 (pg/ml) levels between groups.
Fig. 3: IL-10 (pg/ml) levels between groups.
Fig. 4: Glutathione peroxidases (GP-x) (U/ml) levels between groups.
Fig. 5: Superoxide dismutase (SOD) (U/ml) levels between groups.
Fig. 6: Rate of inflammatory infiltrate and villus changes among SGAs.
Fig. 7: Intestinal sections at 7 dpi stained with H&E showed. A- GIA normal intestinal villi and crypt architecture, B- GIIA short and broad villi (red arrows) with a marked inflammation (yellow arrow) and multiple sections of adults (black arrow), C- GIIIA flattening and fusion of villi (red arrows) with a moderate inflammation (yellow arrow) and sections of adults (black arrow), D- GIVA shortening and blunting of villi (red arrows) with moderate inflammation (yellow arrow) and few sections of adults (black arrow), E- GVA focal broadening of villi (red arrows) with moderate inflammation (yellow arrow), F- GVIA virtually normal architecture with minimal inflammation, G- GVIIA virtually normal architecture with minimal inflammation (X 100 & X 200).

Fig. 8: Muscle sections at 35 dpi. stained with H&E showed. A- GIB normal pattern of skeletal muscle, B- GIIB multiencysted larvae (red arrow) with marked inflammation (yellow arrow), C- GIIIB many viable larvae (red arrow) and moderate inflammation (yellow arrow), D- GIVB few larvae (red arrow) and moderate inflammation (yellow arrows), E- GVB few larvae (red arrows) and moderate inflammation (yellow arrows), F- GVIB nearly normal muscle histology without larvae, G- GVIIB degenerated larvae (red arrow) and minimal inflammatory infiltrate (X 100& X 200).

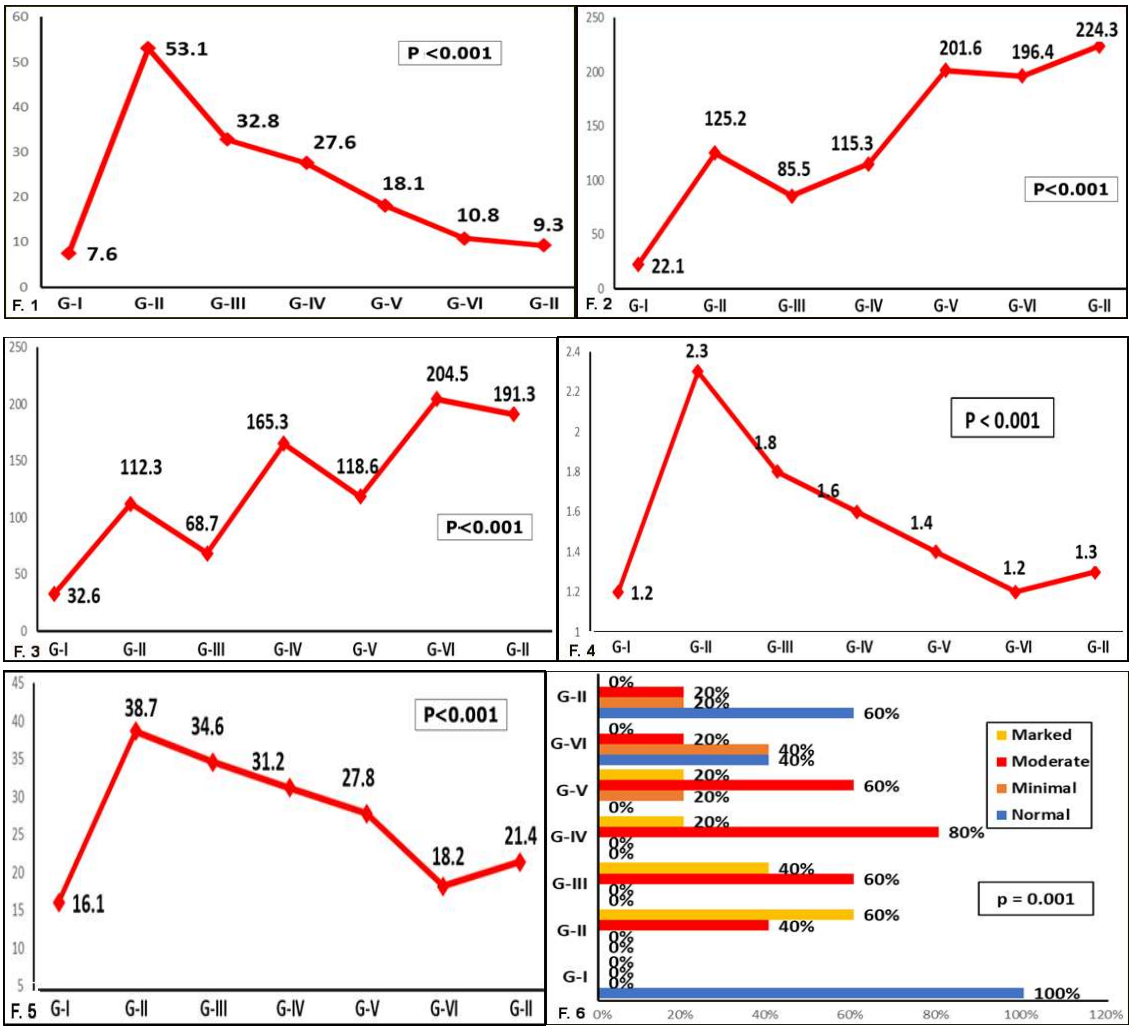

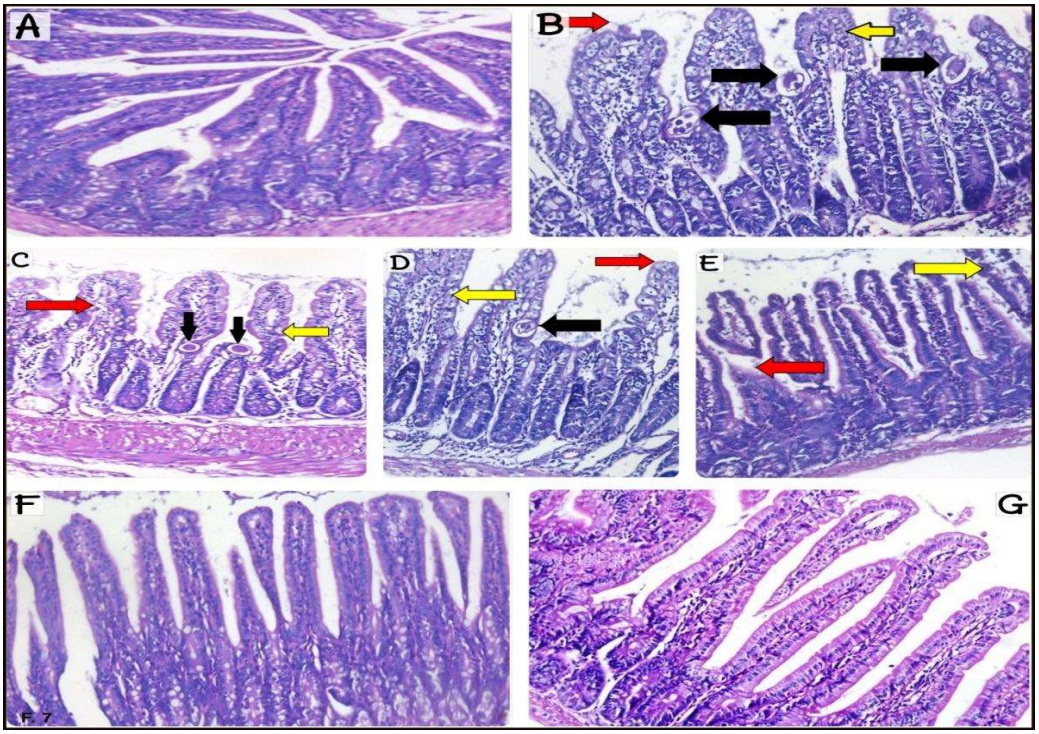
A
B
C
D
E
F
G
F. 7

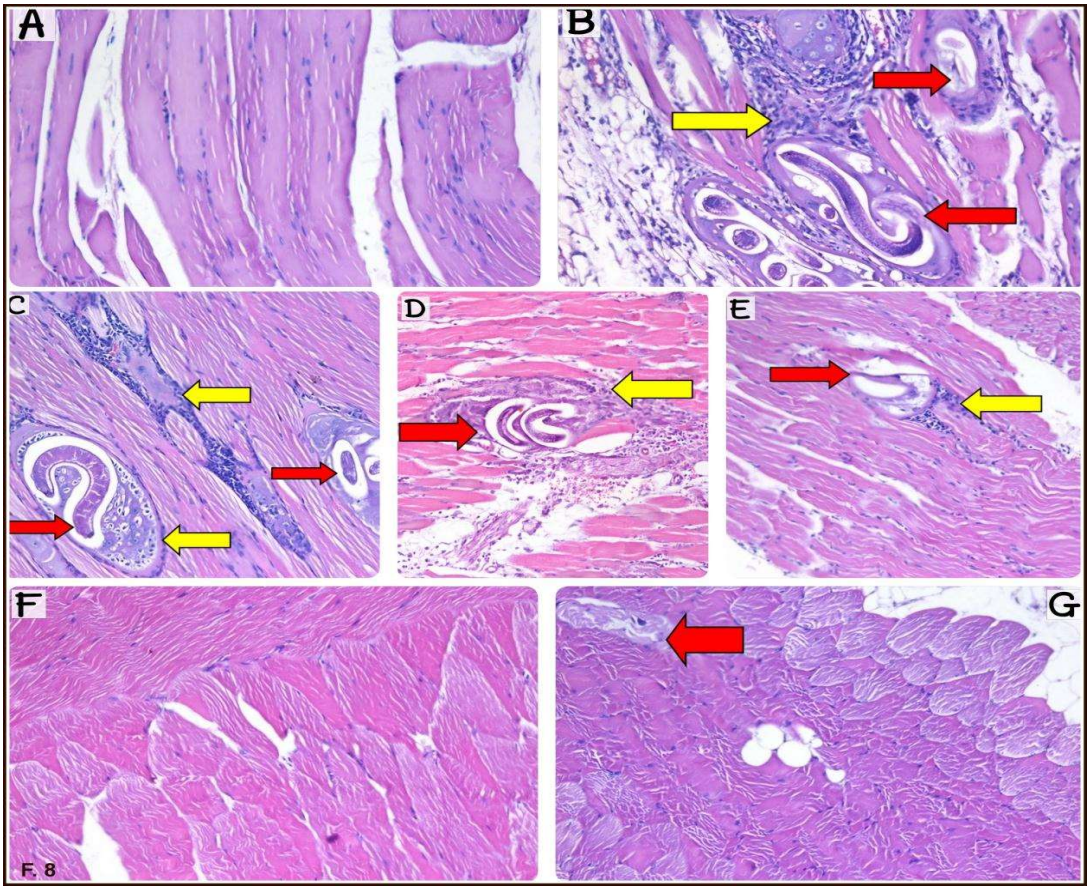
A
B
C
D
E
F
G
F. 8